

THE CARBON MONOXIDE ABUNDANCE IN INTERSTELLAR CLOUDS

WILLIAM LANGER

Institute for Space Studies, Goddard Space Flight Center, NASA;
and Department of Physics, New York University

Received 1975 January 28; revised 1975 November 10

ABSTRACT

We calculate the steady-state abundance of carbon monoxide in interstellar clouds as a function of optical depth, density, and temperature. The molecular reactions which lead to CO can be initiated by the following ion-molecule reactions: $H^+ + O \rightarrow O^+ + H$, $C^+ + H_2 \rightarrow CH_2^+ + h\nu$, and $H_3^+ + C$ and O. As the ultraviolet radiation field is attenuated, C^+ is transformed primarily into CO and C I. There are characteristic column densities for the transition to CO corresponding to the optical depths for attenuating this field at different wavelengths. For thick, low-temperature clouds the attenuation of the fields which ionize carbon, sulfur, and heavy metals is important for CO production initiated by H_3^+ . Complete conversion to CO does not necessarily occur, and considerable neutral carbon may be expected even in optically thick clouds. Comparison of integrated column densities of CO with extinction are in reasonable agreement with observations.

Subject headings: atomic processes — interstellar: molecules

I. INTRODUCTION

The abundances of the heavier trace molecules (i.e., excluding H_2) in interstellar clouds has been discussed and calculated in detail for two regimes: diffuse clouds, and very thick clouds with densities, $n \geq 10^4 \text{ cm}^{-3}$. In diffuse clouds ($A_v \leq 1$) carbon exists primarily as C^+ with trace amounts of C I, CO, CH, CH^+ , H_2CO , and CN (Morton *et al.* 1973). The ultraviolet radiation field, which is not attenuated very much, ionizes carbon ($912 \text{ \AA} < \lambda < 1100 \text{ \AA}$) and photoionizes and dissociates carbon- and oxygen-bearing molecules. The oxygen, which is essentially neutral, is ionized by the slightly endothermic charge exchange, $H^+ + O \rightarrow O^+ + H$ (Field and Steigman 1971). When molecular hydrogen is present in these clouds ion molecule reactions with C^+ (Black and Dalgarno 1973a) and O^+ (Watson 1973, 1974a, b; Dalgarno, Oppenheimer, and Berry 1973; Black and Dalgarno 1973b) eventually lead to CH, CH_2 , C_2H , OH, H_2O , and CO.

In very thick clouds ($A_v \gg 1$), where most of the available carbon or oxygen is probably in CO (Rank, Townes, and Welch 1971; Solomon 1973), there is insufficient radiation ($912 \text{ \AA} < \lambda \leq 3000 \text{ \AA}$) to ionize and dissociate molecules. Here He^+ , H^+ , and H_3^+ are primarily responsible for producing and destroying molecules. These ions are presumed to come from cosmic-ray ionization of He, H, and H_2 . The formation of OH and H_2O , for example, can be initiated by the exothermic reactions $H_3^+ + O \rightarrow OH^+ + H_2$, $H_2O^+ + H$ (Herbst and Klemperer 1973), and similarly for CH and CH_2 by reactions with C.

In this article we consider the abundance of CO and the recombination of C^+ in the transition between diffuse and thick clouds. Some aspects of this transition have been considered by Glassgold and Langer (1975) for warm clouds ($T > 40 \text{ K}$) and at low tem-

peratures by Oppenheimer and Dalgarno (1975). The approach will be to solve the local abundance problem, in the steady state, of the important molecular, atomic, and ionic species as a function of the hydrogen gas density $n = n(H) + 2n(H_2)$, temperature T , cosmic-ray ionization rate $\zeta_p(H)$, and interstellar radiation field $I(\lambda)$. The local abundances are used in the global cloud problem to calculate integrated column densities $N(X)$. The global and local abundance problem are coupled because of the complications of radiation transfer and the effects of self-shielding on the ion abundance.

Reactions involving three different ions can initiate the molecule production chain. These are the following: $H^+ + O \rightarrow O^+ + H$ (Field and Steigman 1971), $C^+ + H_2 \rightarrow CH_2^+ + h\nu$ (Black and Dalgarno 1973a), and $H_3^+ + O \rightarrow H_2O^+ + H$, $OH^+ + H_2$ (Herbst and Klemperer 1973) and $H_3^+ + C \rightarrow CH_2^+ + H$, $CH^+ + H_2$. The abundances of these ions determine the rate of molecule formation, the H^+ and H_3^+ abundances depend on the cosmic-ray ionization rate, and the C^+ and H_3^+ (which is destroyed by dissociative recombination with electrons) abundances depend on $I(\lambda)$. There will be different transition regions for molecule production via these reactions corresponding to the characteristic optical depths for attenuating the ultraviolet radiation field which photodissociates molecules and photoionizes atoms. In thicker clouds the photoionization of sulfur and heavy metals is important, since they can be major components of $n(e)$, and $n(H_3^+) \propto n_e^{-1}$. Furthermore, we suggest that the formation of C_2 enhances significantly the CO abundance because of its likely small photodissociation rate.

We discuss the conditions of temperature, density, and position into a cloud where each of these mechanisms dominates for producing CO. The C^+ does not always recombine entirely into CO as the radiation

field is attenuated, but mixtures of C I and CO (with trace amounts of C_2H , CH , CH_2 , C_2 , etc.) exist. When $T \lesssim 30$ K and $n \lesssim 10^3 \text{ cm}^{-3}$, significant amounts of neutral carbon will be present, even in thick clouds. Finally, these abundance calculations are compared with recent measurements in dark clouds of the CO column density as a function of extinction (Encrenaz, Falgarone, and Lucas 1975; Dickman 1975).

II. CALCULATION

The C^+ recombination problem discussed by Werner (1970) considered only radiative recombination as a loss mechanism. Ion-molecule reactions in regions containing mainly molecular hydrogen (i.e., when $N \gtrsim 2 \times 10^{20} \text{ cm}^{-2}$), however, can dominate C^+ recombination (Glassgold and Langer 1975). The three main destruction mechanisms for C^+ are the following: (1) radiative recombination, $C^+ + e \rightarrow C + h\nu$; (2) radiative association, $C^+ + H_2 \rightarrow CH_2^+ + h\nu$ (Black and Dalgarno 1973a) and $C^+ + H \rightarrow CH^+ + h\nu$ (Solomon and Klemperer 1972); and (3) ion-molecule reactions with the most abundant carbon- and oxygen-bearing molecules— OH , H_2O , CH , and CH_2 . In diffuse clouds, or the outer regions of thick clouds, radiative recombination dominates, but as the ultraviolet radiation field is attenuated the second and/or third mechanisms dominate.

The two main mechanisms for production of CO are ion-molecule and neutral molecule reactions. In the former case the C^+ interacts with OH and H_2O to produce CO either directly or indirectly (Glassgold and Langer 1975, 1976b) at a characteristic ion-molecule reaction rate, $k' \approx 2 \times 10^{-9} \text{ cm}^3 \text{ s}^{-1}$. The neutral molecule reactions are the following: $CH + O \rightarrow HCO^+ + e$, rate constant $a_3 = 10^{-11}-10^{-10} \text{ cm}^3 \text{ s}^{-1}$ (Dalgarno, Oppenheimer, and Berry 1973); $C_2H + O \rightarrow CH + CO$ (Watson 1974a), $a_6 = 4 \times 10^{-11} \text{ cm}^3 \text{ s}^{-1}$; $C + OH \rightarrow CO + H$ (Herbst and Klemperer 1973), $a_1 = 4 \times 10^{-11} \text{ cm}^3 \text{ s}^{-1}$; and $C_2 + O \rightarrow CO + C$ (Solomon and Klemperer 1972), $a_7 = 4 \times 10^{-11} \text{ cm}^3 \text{ s}^{-1}$. This last rate is highly uncertain and might be considerably smaller ($\sim 10^{-13} \text{ cm}^3 \text{ s}^{-1}$), however, as discussed in the Appendix; this uncertainty will not make a significant difference in the CO abundance. It is therefore necessary to understand the production mechanisms of OH , H_2O , CH , CH_2 , C_2H , and C_2 and the regimes where each dominates to calculate the CO abundance (and the C^+ recombination). Throughout this work we use the notation and rates established in the recent paper on the ionization balance and the formation of oxygen-bearing molecules in diffuse clouds by Glassgold and Langer (1976b). In Tables 1–3 we have listed the additional reactions needed to solve completely the CO problem in interstellar clouds; these include the reactions for producing and destroying the CH and C_2H family and O_2 , reactions involving H_3^+ , and reactions of sulfur and the heavy metals.

The slightly endothermic charge exchange $H^+ + O \rightarrow O^+ + H$, $k_5 = 10^{-9} \exp(-232/T) \text{ cm}^3 \text{ s}^{-1}$ (Field and Steigman 1971) begin a series of reactions which

end in OH and H_2O (Watson 1973, 1974a; Dalgarno, Oppenheimer, and Berry 1973; Black and Dalgarno 1973b). This reaction is followed by the ion-molecule reactions $O^+ + H_2 \rightarrow OH^+ + H$, $OH^+ + H_2 \rightarrow H_2O^+ + H$, and $H_2O^+ + H_2 \rightarrow H_3O^+ + H$; by dissociative recombinations $H_3O^+ + e \rightarrow H_2O + H$ and $OH + H_2$; and by photodissociation of H_2O . The exothermic reactions $H_3^+ + O \rightarrow OH^+ + H_2$, $H_2O^+ + H$ (Herbst and Klemperer 1973) also initiate the chain of reactions leading to OH and H_2O . In thick, dense clouds Herbst and Klemperer (1973) proposed that, through these reactions with O and C, the H_3^+ is the progenitor of molecule formation. Because their reaction rates, $k \approx 2 \times 10^{-9} \text{ cm}^3 \text{ s}^{-1}$, are not sensitive to temperature, as is the $H^+ + O$ charge exchange, at sufficiently low temperatures H_3^+ dominates the formation of OH and H_2O .

The H_3^+ ion also interacts with C I to form the CH family of molecules (CH , CH_2 , C_2H , etc.), $H_3^+ + C \rightarrow CH^+ + H_2$, $CH_2^+ + H$ (Herbst and Klemperer 1973) at a rate of $\sim 10^{-9} \text{ cm}^3 \text{ s}^{-1}$. These reactions are followed by $CH^+ + H_2 \rightarrow CH_2^+ + H$ and $CH_2^+ + H_2 \rightarrow CH_3^+ + H$; by dissociative recombinations $CH_3^+ + e \rightarrow CH_2 + H$ and $CH + H_2$; and by photodissociation of CH_2 . The C_2H molecule is formed by the ion-molecule reactions (Watson 1974a, b) $C^+ + CH \rightarrow C_2^+ + H$, $C_2^+ + H_2 \rightarrow C_2H^+ + H$, $C_2H^+ + H_2 \rightarrow C_2H_2^+ + H$ with typical rates of $\sim 10^{-9} \text{ cm}^3 \text{ s}^{-1}$; and by dissociative recombination $C_2H_2^+ + e \rightarrow C_2H + H$, with a rate $\beta_{11}(C_2H_2^+) \approx 10^{-6} \text{ cm}^3 \text{ s}^{-1}$. The C_2 molecule is produced by photo-dissociation of C_2H , $h\nu + C_2H \rightarrow C_2 + H$, and dissociative charge exchange with He^+ .

The final gas phase reaction which initiates molecule production is radiative association of C^+ with molecular hydrogen (Black and Dalgarno 1973a). Radiative association with H, $C^+ + H \rightarrow CH^+ + h\nu$ (Solomon and Klemperer 1972), will not be included, since this paper is concerned with regions containing large fractional abundances of H_2 [$f = 2n(H_2)/n \geq 0.8$] characteristic of clouds with column densities $N \gtrsim 10^{21} \text{ cm}^{-2}$ (Glassgold and Langer 1974; Spitzer *et al.* 1973). Unfortunately, the rate, $k_{26}(CH_2^+)$, for the radiative association mechanism $C^+ + H_2 \rightarrow CH_2^+ + h\nu$, is not well known. Black and Dalgarno (1973a) estimated that, to explain the CH abundance in ζ Oph, this rate would have to lie in the range 3×10^{-16} to $2 \times 10^{-15} \text{ cm}^3 \text{ s}^{-1}$, with the larger rate corresponding to carbon depletion by a factor of 10. To explain measured column densities of CH^+ in a large number of diffuse clouds, Black, Dalgarno, and Oppenheimer (1975) suggest that a rate of $10^{-14} \text{ cm}^3 \text{ s}^{-1}$ may be necessary. From three-body association rates of C^+ with H_2 in He, Fehsenfeld, Dunkin, and Ferguson (1974) estimated a radiative association rate of $\sim 4 \times 10^{-17} \text{ cm}^3 \text{ s}^{-1}$ at 90 K. Herbst (1975) suggests a rate of $\sim 10^{-16} \text{ cm}^3 \text{ s}^{-1}$ for this reaction. In this work we take the point of view that there are too many uncertainties in density, radiation field, photoionization and dissociation rates, and branching ratios in the theory, and that the experiment does not measure the two-body rate directly, to fix this rate at this time.

TABLE 1
CARBON MOLECULE FAMILY REACTIONS

Reaction	Rate ($\text{cm}^{-3} \text{s}^{-1}$)	Reference*
<i>Radiative association:</i>		
$\text{C}^+ + \text{H}_2 \rightarrow \text{CH}_2^+ + h\nu$	$k_{26} = 10^{-16}-10^{-14}$	1,7
<i>Ion-molecule:</i>		
$\text{CH}_2^+ + \text{H}_2 \rightarrow \text{CH}_3^+ + \text{H}$	$k_{27} = 7 \times 10^{-10}$	9
$\text{CH}^+ + \text{H}_2 \rightarrow \text{CH}_2^+ + \text{H}$	$k_{28} = 10^{-9}$	9
$\text{C}^+ + \text{CH} \rightarrow \text{C}_2^+ + \text{H}$	$k_{29} = 2 \times 10^{-9}$	2
$\text{C}_2^+ + \text{O} \rightarrow \text{CO} + \text{C}^+$	$k_{30} = 10^{-9}$	3
$\text{CH}_3^+ + \text{O} \rightarrow \text{H}_2\text{CO}^+ + \text{H}$	$k_{31} = 2 \times 10^{-9}$	8
$\text{C}^+ + \text{O}_2 \rightarrow \text{CO}^+ + \text{O}$	$k_{32} = 10^{-9}$	2
$\text{C}^+ + \text{O}_2 \rightarrow \text{CO} + \text{O}^+$	$k_{33} = 10^{-9}$	
$\text{C}^+ + \text{H}_2\text{CO} \rightarrow \text{HC}_2\text{O}^+ + \text{H}$	$k_{34} = 2 \times 10^{-9}$	2
$\text{C}^+ + \text{CH}_2 \rightarrow \text{C}_2\text{H}^+ + \text{H}$	$k_{35} = 2 \times 10^{-9}$	2
$\text{C}^+ + \text{CH}_3 \rightarrow \text{C}_2\text{H}_2^+ + \text{H}$	$k_{36} = 10^{-9}$	7
$\text{C}_2^+ + \text{H}_2 \rightarrow \text{C}_2\text{H}^+ + \text{H}$	$k_{37} = 1.1 \times 10^{-9}$	9
$\text{C}_2\text{H}^+ + \text{H}_2 \rightarrow \text{C}_2\text{H}_2^+ + \text{H}$	$k_{38} = 8 \times 10^{-10}$	9
<i>Charge exchange:</i>		
$\text{C} + \text{O}_2^+ \rightarrow \text{C}^+ + \text{O}_2$	$k_{39} = 10^{-9}$	2
$\text{H}^+ + \text{CH} \rightarrow \text{CH}^+ + \text{H}$	$k_{40} = 10^{-9}$	
$\text{H}^+ + \text{CH}_2 \rightarrow \text{CH}_2^+ + \text{H}$	$k_{41} = 10^{-9}$	
$\text{H}^+ + \text{C}_2\text{H} \rightarrow \text{C}_2\text{H}^+ + \text{H}$	$k_{42} = 10^{-9}$	
$\text{H}^+ + \text{C}_2 \rightarrow \text{C}_2^+ + \text{H}$	$k_{43} = 10^{-9}$	
$\text{H}^+ + \text{HCO} \rightarrow \text{HCO}^+ + \text{H}$	$k_{44} = 10^{-9}$	
$\text{H}^+ + \text{H}_2\text{CO} \rightarrow \text{H}_2\text{CO}^+ + \text{H}$	$k_{45} = 10^{-9}$	
$\text{H}_2\text{CO}^+ + (\text{M}, \text{S}) \rightarrow \text{H}_2\text{CO} + (\text{M}^+, \text{S}^+)^\dagger$	$k_{46} = 2 \times 10^{-9}$	10
$\text{CH}_3^+ + \text{M} \rightarrow \text{CH}_3 + \text{M}^+$	$k_{47} = 10^{-9}$	
$\text{He}^+ + (\text{CH}, \text{CH}_2, \text{C}_2\text{H}, \text{C}_2) \rightarrow \text{He} + \text{all channels}$	$k_{48} = 5 \times 10^{-10}$	
$\text{He}^+ + (\text{CH}, \text{C}_2) \rightarrow \text{He} + (\text{C} + \text{H}^+, \text{C} + \text{C}^+)$	$k_{49} = 3 \times 10^{-10}$	
<i>Dissociative recombination:</i> ‡		
$\text{CH}_2^+ + e \rightarrow \text{CH} + \text{H}$	$\beta_7 = 5 \times 10^{-7}$	7,8
$\text{CH}_3^+ + e \rightarrow \text{all products}$	$\beta_8 = 10^{-6}$	10
$\rightarrow \text{CH}_2 + \text{H}$	$\beta_9(\text{CH}_2)$	
$\rightarrow \text{CH} + \text{H}_2$	$\beta_{10}(\text{CH})$	
$\rightarrow \text{CH}_3 + h\nu$	$\beta_{11}(\text{CH}_3) = 3 \times 10^{-10}$	7
$\text{H}_3\text{CO}^+ + e \rightarrow \text{all channels}$	$\beta_9 = 2 \times 10^{-6}$	2
$\text{H}_2\text{CO}^+ + e \rightarrow \text{CO} + (\text{H}_2 \text{ or } 2\text{H})$	$\beta_{10} = 6 \times 10^{-7}$	2
$\text{C}_2\text{H}_2^+ + e \rightarrow \text{C}_2\text{H} + \text{H}$	$\beta_{11} = 10^{-6}$	
$\text{CH}^+ + e \rightarrow \text{C} + \text{H}$	$\beta_{12} = 10^{-7}$	5
$\text{C}_2^+ + e \rightarrow \text{C} + \text{C}$	$\beta_{13} = 5 \times 10^{-7}$	
$\text{C}_2\text{H}^+ + e \rightarrow \text{C}_2 + \text{H}$	$\beta_{14} = 5 \times 10^{-7}$	
<i>H_3^+ Ion-molecule:</i>		
$\text{H}_3^+ + \text{C} \rightarrow \text{CH}^+ + \text{H}_2$	$K_5 = 2 \times 10^{-9}$	2
$\text{H}_3^+ + \text{C} \rightarrow \text{CH}_2^+ + \text{H}$	$K_6 = 10^{-9}$	
$\text{H}_3^+ + \text{CO} \rightarrow \text{HCO}^+ + \text{H}_2$	$K_7 = 1.4 \times 10^{-9}$	2
$\text{H}_3^+ + \text{C}_2 \rightarrow \text{C}_2\text{H}^+ + \text{H}_2$	$K_8 = 10^{-9}$	
<i>Neutral molecule:</i>		
$\text{C} + \text{OH} \rightarrow \text{CO} + \text{H}$	$a_2 = 4 \times 10^{-11}$	2
$\text{CH} + \text{O} \rightarrow \text{HCO}^+ + e$	$a_3 = 10^{-11}-10^{-10}$	4
$\text{CH}_2 + \text{O} \rightarrow \text{HCO} + \text{H}$	$a_4 = 4 \times 10^{-11}$	8
$\text{CH}_3 + \text{O} \rightarrow \text{H}_2\text{CO} + \text{H}$	$a_5 = 3 \times 10^{-11}$	10
$\text{C}_2\text{H} + \text{O} \rightarrow \text{CO} + \text{CH}$	$a_6 = 4 \times 10^{-11}$	5
$\text{C}_2 + \text{O} \rightarrow \text{CO} + \text{C}$	$a_7 = 10^{-11}-4 \times 10^{-11}$	3
<i>Photodestruction:</i>		
$h\nu + \text{CH} \rightarrow \text{CH}^+ + e$	$G_i(\text{CH}) = 10^{-10} \text{ s}^{-1}$	1
$h\nu + \text{CH} \rightarrow \text{C} + \text{H}$	$G_d(\text{CH}) = 2 \times 10^{-10} \text{ s}^{-1}$	1
$h\nu + \text{CH}_2 \rightarrow \text{all channels}$	$G(\text{CH}_2) \simeq 10^{-10} \text{ s}^{-1}$	8
$h\nu + \text{CH}_3 \rightarrow \text{all channels}$	$G(\text{CH}_3) \simeq 10^{-10} \text{ s}^{-1}$	
$h\nu + \text{C}_2\text{H} \rightarrow \text{all channels}$	$G(\text{C}_2\text{H}) \simeq 10^{-10} \text{ s}^{-1}$	
$h\nu + \text{C}_2 \rightarrow \text{C} + \text{C}$	$G_d(\text{C}_2) = 10^{-11} \text{ s}^{-1}$	
$h\nu + \text{C}_2 \rightarrow \text{C}_2^+ + e$	$G(\text{C}_2) = 10^{-10} \text{ s}^{-1}$	
$h\nu + \text{CO} \rightarrow \text{C} + \text{O}$	$G(\text{CO}) = 10^{-11} \text{ s}^{-1}$	11

* Numerical values of rate constants without references have been estimated or guessed.

† Here M denotes the heavy metals, Mg, Fe, Si, etc., and S is sulfur.

‡ The notation β_8 indicates, for example, the total recombination rate to all channels. When the branch $\text{CH}_3^+ + e \rightarrow \text{CH}_2 + \text{H}$ is required, its rate constant is denoted as $\beta_8(\text{CH}_2)$. A similar notation applies to photoprocesses.

REFERENCES FOR TABLES 1-3.—(1) Black and Dalgarno 1973a. (2) Herbst and Klemperer 1973. (3) Solomon and Klemperer 1972. (4) Dalgarno *et al.* 1973. (5) Watson 1974a, b. (6) Oppenheimer and Dalgarno 1974a. (7) Black *et al.* 1975. (8) Dalgarno and Oppenheimer 1974. (9) Kim *et al.* 1975. (10) Dalgarno *et al.* 1973. (11) Glassgold and Langer 1976b. (12) Oppenheimer and Dalgarno 1974b. (13) de Boer *et al.* 1973.

TABLE 2
OXYGEN MOLECULE FAMILY REACTIONS

Reaction	Rate ($\text{cm}^3 \text{s}^{-1}$)	Reference*
<i>Radiative association:</i>		
$\text{HCO}^+ + \text{H}_2 \rightarrow \text{H}_3\text{CO}^+ + h\nu$	$k_{50} = 10^{-17}$	2
<i>Ion-molecule:</i>		
$\text{HCO}^+ + \text{OH} \rightarrow \text{HCO}_2^+ + \text{H}$	$k_{51} = 10^{-9}$	2
$\text{HCO}^+ + \text{H}_2\text{O} \rightarrow \text{H}_3\text{O}^+ + \text{CO}$	$k_{52} = 5 \times 10^{-10}$	2
<i>Charge exchange:</i>		
$\text{H}^+ + \text{O}_2 \rightarrow \text{O}_2^+ + \text{H}$	$k_{53} = 10^{-9}$	2
$\text{He}^+ + \text{O}_2 \rightarrow \text{O}_2^+ + \text{He}$	$k_{54} = 3.8 \times 10^{-10}$	2
<i>Dissociative charge exchange:</i>		
$\text{He}^+ + \text{O}_2 \rightarrow \text{O}^+ + \text{O} + \text{He}$	$k_{55} = 6.2 \times 10^{-10}$	2
$\text{He}^+ + (\text{OH}, \text{H}_2\text{O}) \rightarrow \text{He} + (\text{O} + \text{H}^+, \text{etc.})$	$k_{56} \approx 3 \times 10^{-10}$	
<i>Dissociative recombination:</i>		
$\text{O}_2^+ + e \rightarrow \text{O} + \text{O}$	$\beta_{18} = 2 \times 10^{-7}$	2
<i>H_3^+ Ion-molecule:</i>		
$\text{H}_3^+ + \text{O} \rightarrow \text{H}_2\text{O}^+ + \text{H}$	$K_1 = 10^{-9}$	
$\text{H}_3^+ + \text{O} \rightarrow \text{OH}^+ + \text{H}_2$	$K_2 = 2 \times 10^{-9}$	2
$\text{H}_3^+ + \text{OH} \rightarrow \text{H}_2\text{O}^+ + \text{H}_2$	$K_3 = 2 \times 10^{-9}$	2
$\text{H}_3^+ + \text{H}_2\text{O} \rightarrow \text{H}_3\text{O}^+ + \text{H}_2$	$K_4 = 3 \times 10^{-9}$	2
<i>Neutral molecule:</i>		
$\text{O} + \text{OH} \rightarrow \text{O}_2 + \text{H}$	$a_1 = 5 \times 10^{-11}$	2
<i>Photodestruction:</i>		
$h\nu + \text{O}_2 \rightarrow \text{all channels}$	$G(\text{O}_2) = 10^{-11} \text{ s}^{-1}$	

* See Table 1. Numerical values of rate constants without references have been estimated or guessed.

Instead we explore the consequences of different radiative association rates on CO and C⁺ abundance.

It is clear from the previous discussion that the abundance of the ions C⁺, H⁺, and H₃⁺ controls molecule production. The H⁺ abundance will depend on density n , cosmic-ray ionization rate ζ_p , and temperature. The C⁺ can be expected to be important up to some characteristic optical depth at which the ultraviolet radiation in the range, $912 \text{ \AA} < \lambda \lesssim 1100 \text{ \AA}$, is attenuated enough to cease ionizing the carbon. The H₃⁺ abundance increases with attenuation of the ultraviolet radiation that ionizes carbon, sulfur, and the heavy metals. These ions contribute significantly to the electrons, which are the dominant destruction mechanism for H₃⁺ [dissociative recombination at a rate $\beta_1(\text{H}_3^+) \approx 2 \times 10^{-6} T^{-0.5} \text{ cm}^3 \text{ s}^{-1}$].

The sulfur and heavy metal atoms remain ionized to much larger distances into clouds than carbon because they are ionized by a wider range of photon energies with characteristically smaller grain extinction (see also Walmsley 1973). There can be different characteristic transition regions for molecule production because of these effects. Similarly, there are different density and temperature regimes where either C⁺ or H⁺ dominate.

The elements of the steady-state, local CO abundance in interstellar clouds are the following: (1) the balance equations for all important oxygen- and carbon-containing species, to yield the abundances of OH, H₂O, O₂, CH, CH₂, C₂H, C₂, and CO; (2) the ionization balance, to yield the abundances of H⁺, H₃⁺, He⁺, C⁺, S⁺, Si⁺, Mg⁺, Fe⁺; (3) the conservation conditions for the total amount of oxygen,

carbon, sulfur, and the heavy metals in gaseous form; and (4) specification of ζ_p and $I(\lambda)$. We will ignore density and temperature inhomogeneities and assume for purposes of calculation that n and T are constant. Many of the details involved in constructing the steady-state balance equations have been presented in Glassgold and Langer (1976b). We shall omit these detailed considerations but note that, as in Glassgold and Langer (1975) on the C⁺-CO transition in warm clouds, many of the low-abundance members of the carbon and oxygen families can be eliminated from the coupled rate equations to yield simplified balance equations for the dominant molecules. In Appendix A we discuss the balance equations for these molecules, excluding CO which is discussed below, and the ions H⁺, H₃⁺, and He⁺. For the CO fractional abundance we find

$$x(\text{CO}) = \{k'x(\text{C}^+)x_M(\text{O}) + [a_3x(\text{CH}) + a_4x(\text{CH}_2) + a_6x(\text{C}_2\text{H}) + a_7x(\text{C}_2)]x(\text{O})\}/[g(\text{CO}) + k_{25}x(\text{He}^+)] \quad (1)$$

where production is either directly or indirectly via C⁺ interacting with the oxygen-bearing molecules $x_M(\text{O}) = x(\text{OH}) + x(\text{H}_2\text{O}) + x(\text{O}_2)$ at a characteristic ion-molecule rate, $k' = 2 \times 10^{-9} \text{ cm}^3 \text{ s}^{-1}$, or by neutral molecule reactions of oxygen with the CH family and C₂. For CH₂ and C₂H the characteristic reaction rate is $a_4 \approx a_6 \approx a' = 4 \times 10^{-11} \text{ cm}^3 \text{ s}^{-1}$, while the rate a_3 for the chemi-ionization of CH has been estimated to be $\sim 10^{-11}-10^{-10} \text{ cm}^3 \text{ s}^{-1}$ (Dalgarno, Oppenheimer, and Berry 1973). We choose an

TABLE 3
SULFUR AND METAL REACTIONS

Reaction	Rate ($\text{cm}^3 \text{s}^{-1}$)	Reference*
<i>Radiative association:</i>		
$\text{Si}^+ + \text{H}_2 \rightarrow \text{SiH}_2^+ + h\nu$	$k_{57} = 10^{-16}$	
<i>Ion-molecule:</i>		
$\text{Si}^+ + \text{O}_2 \rightarrow \text{SiO}^+ + \text{O}$	$k_{58} = 10^{-9}$	
$\text{Si}^+ + \text{OH} \rightarrow \text{SiO}^+ + \text{H}$	$k_{59} = 10^{-9}$	
$\text{C}^+ + \text{SiO} \rightarrow \text{CO} + \text{Si}^+$	$k_{60} = 10^{-9}$	
$\text{H}_2\text{S}^+ + \text{O} \rightarrow \text{SH}^+ + \text{OH}$	$k_{61} = 10^{-9}$	
$\text{SH}^+ + \text{O} \rightarrow \text{SO}^+ + \text{H}$	$k_{62} = 10^{-9}$	6
$\text{SH}^+ + \text{O} \rightarrow \text{S}^+ + \text{OH}$	$k_{63} = 10^{-9}$	6
$\text{C}^+ + \text{SO} \rightarrow \text{S}^+ + \text{CO}$	$k_{64} = 10^{-9}$	6
<i>Charge-exchange:</i>		
$\text{Si}^+ + \text{Mg} \rightarrow \text{Si} + \text{Mg}^+$	$k_{65} = 2 \times 10^{-9}$	
$\text{Si}^+ + \text{Fe} \rightarrow \text{S} + \text{Fe}^+$	$k_{66} = 3 \times 10^{-9}$	
$\text{SH}^+ + (\text{Mg}, \text{S}, \text{Si}) \rightarrow \text{SH} + (\text{Mg}^+, \text{S}^+, \text{Si}^+)$	$k_{67} = 10^{-10}$	6
$\text{H}_2\text{S}^+ + (\text{Mg}, \text{S}, \text{Si}) \rightarrow \text{H}_2\text{S} + (\text{Mg}^+, \text{S}^+, \text{Si}^+)$	$k_{68} = 10^{-10}$	6
$\text{SO}^+ + \text{Mg} \rightarrow \text{SO} + \text{Mg}^+$	$k_{69} = 10^{-10}$	6
$\text{H}^+ + \text{SH} \rightarrow \text{SH}^+ + \text{H}$	$k_{70} = 10^{-9}$	
$\text{H}^+ + \text{H}_2\text{S} \rightarrow \text{H}_2\text{S}^+ + \text{H}$	$k_{80} = 10^{-9}$	
$\text{HCO}^+ + (\text{Mg}, \text{Si}, \text{Fe}) \rightarrow \text{HCO} + (\text{Mg}^+, \text{Si}^+, \text{Fe}^+)$	$k_{81} = 10^{-9}$	
$\text{O}_2^+ + (\text{Mg}, \text{Si}, \text{S}, \text{Fe}) \rightarrow \text{O}_2 + (\text{Mg}^+, \text{Si}^+, \text{S}^+, \text{Fe}^+)$	$k_{82} = 10^{-9}$	
<i>Dissociative recombination:</i>		
$\text{SH}^+ + e \rightarrow \text{S} + \text{H}$	$\beta_{15} = 10^{-7}$	6
$\text{H}_2\text{S}^+ + e \rightarrow \text{SH} + \text{H}$	$\beta_{16} = 10^{-6}$	6
$\text{SiO}^+ + e \rightarrow \text{Si} + \text{O}$	$\beta_{17} = 3 \times 10^{-7}$	
<i>Radiative recombination:</i>		
$(\text{S}^+, \text{Si}^+, \text{Fe}^+, \text{Mg}^+) + e \rightarrow (\text{S}, \text{Si}, \text{Fe}, \text{Mg}) + h\nu$	$\alpha = 1.9 \times 10^{-10} T^{-0.7}$	
<i>H₃⁺ Ion-molecule:</i>		
$\text{H}_3^+ + (\text{Mg}, \text{Fe}, \text{Si}) \rightarrow (\text{Mg}^+, \text{Fe}^+, \text{Si}^+) + \text{H}_2 + \text{H}$	$k_9 = 10^{-9}$	11
$\text{H}_3^+ + \text{S} \rightarrow \text{SH}^+ + \text{H}_2$	$k_{10} = 2 \times 10^{-9}$	6
$\text{H}_3^+ + \text{S} \rightarrow \text{SH}_2^+ + \text{H}$	$k_{11} = 2 \times 10^{-9}$	6
$\text{H}_3^+ + \text{SH} \rightarrow \text{SH}_2^+ + \text{H}_2$	$k_{12} = 10^{-9}$	6
<i>Neutral molecule:</i>		
$\text{SH} + \text{O} \rightarrow \text{SO} + \text{H}$	$a_8 = 2 \times 10^{-10}$	6
<i>Photodestruction:</i>		
$h\nu + \text{S} \rightarrow \text{S}^+ + e^-$	$G(\text{S}) = 9.6 \times 10^{-10} \text{ s}^{-1}$	13
$h\nu + \text{Mg} \rightarrow \text{Mg}^+ + e^-$	$G(\text{Mg}) = 3.7 \times 10^{-11} \text{ s}^{-1}$	13
$h\nu + \text{Fe} \rightarrow \text{Fe}^+ + e^-$	$G(\text{Fe}) = 1.5 \times 10^{-10} \text{ s}^{-1}$	13
$h\nu + \text{Si} \rightarrow \text{Si}^+ + e^-$	$G(\text{Si}) = 1.7 \times 10^{-9} \text{ s}^{-1}$	13
$h\nu + (\text{SH}, \text{SH}_2) \rightarrow \text{all channels}$	$G(\text{SH}_x) \approx 10^{-10} \text{ s}^{-1}$	
$h\nu + \text{SO} \rightarrow \text{S} + \text{O}$	$G(\text{SO}) = 10^{-10} \text{ s}^{-1}$	
$h\nu + \text{SiO} \rightarrow \text{Si} + \text{O}$	$G(\text{SiO}) = 10^{-10} \text{ s}^{-1}$	

* See Table 1. Numerical values of rate constants without references have been estimated or guessed.

intermediate value, $a_3 \approx a'$ for convenience. Even though C₂ is not a radical its ${}^1\Sigma$ state does not look like a closed shell, and we adopt the typical value suggested by Solomon and Klemperer (1972), $a_7 \approx 3 \times 10^{-11} \text{ cm}^3 \text{s}^{-1}$. Even if this reaction rate is much smaller it will not affect significantly the results in the transition region (see Appendix A). Omitted from equation (1) are negligible reactions (e.g., C + OH → CO + H), as well as destruction terms which essentially cancel production terms. For example, the reaction $\text{H}_3^+ + \text{CO} \rightarrow \text{HCO}^+ + \text{H}_2$, destroys CO; however, HCO⁺ recombinations with electrons [rate $\beta_6(\text{HCO}^+) \sim 3 \times 10^{-7} \text{ cm}^3 \text{s}^{-1}$ at $T = 200 \text{ K}$, and possibly larger at lower temperatures, Herbst and Klemperer 1973] leading to CO will dominate HCO⁺ destruction for $x_e \geq 2 \times 10^{-7}$. For the regions of interest in this paper this condition is satisfied.

Equation (1) and the balance equations in Appen-

dices A and B must be supplemented by charge conservation

$$x_e = \sum_i x_i(\text{X}^+). \quad (2)$$

The most important ions, $x_i(\text{X}^+)$, are C⁺, H⁺, He⁺, S⁺, M⁺ (metal ions), and H₃⁺, with significant contributions to the electron abundance from H₃O⁺ and HCO⁺ at high densities ($n > 10^4 \text{ cm}^{-3}$). Ionized carbon is the main source of electrons in the H₂ regions of clouds where the ultraviolet radiation field is not attenuated much. Beyond this region in the interiors of clouds with significant (but not total) extinction such that the carbon is primarily atomic or molecular, H⁺, M⁺, and S⁺ are the major ions. The metals (e.g., Si, Mg, Fe) and sulfur are important sources of electrons in these regions because they do not, as ions, engage readily in ion-molecule reactions

(Oppenheimer and Dalgarno 1974b). They can remain ionized deep into clouds because they are destroyed by the relatively slow radiative recombination process, have ionization potentials less than that of carbon, sometimes charge exchange with metals having lower ionization potentials (see Table 3), and in the case of the metals can be produced by charge exchange with H_3^+ . The chemical balance equations for S, Si, Mg, and Fe are discussed in Appendix B. We neglect the metals, Al, Ca, Na, and Cl because of their small abundance compared with Mg, Fe, and Si (Morton *et al.* 1973).

With regard to the global aspects of the abundance problem we assume, except for photoionization of carbon, sulfur, and the metals, that photodissociation and ionization rates vary with optical depth into the cloud as $G(X) \approx G_0(X) \exp[-\tau_g(X)]$. The photo-destruction rate at zero optical depth is given by $G_0(X)$, and $\tau_g(X) = N\sigma_{gr}(X)$ is a mean grain attenuation for the relevant energy range. The optical depths for grain attenuation of the ultraviolet radiation field are estimated from the analysis of Glassgold and Langer (1974), based on ultraviolet extinction data. The relevant values of $\tau_g(X)$ are listed in Table 4; in § IV we discuss the effect on the transition of assuming a different grain albedo.

For carbon, sulfur, and the metals, self-shielding can be important for recombination, and generally sharpens the transition between regimes where different CO production mechanisms dominate. For carbon the photoionization is given by $G(X) \approx G_0(X)e^{-\tau(C)}$, with

$$\tau(C) = \tau_g(C) + N(C) \int_{912}^{1100} \sigma_c(\lambda) d\lambda, \quad (3)$$

where $\tau_g(C) = N\sigma_{gr}(C) \approx N(8 \times 10^{20} \text{ cm}^{-2})^{-1}$ is the mean grain attenuation. The self-shielding due to the neutral carbon is given by the second term in $\tau(C)$ (Werner 1970) where $N(C)$ is the column density of neutral carbon toward a point x in a one-dimensional slab model of a cloud. For the carbon photoionization cross section we use $\sigma_c(\lambda) \approx 1.1 \times 10^{-17} \text{ cm}^2$ (McGuire 1968). The photoionization rate of sulfur and silicon is given by a similar expression with

$$\tau(X) = \tau_g(X) + N(X) \int_{912}^{\lambda_{th}} \sigma_x(\lambda) d\lambda. \quad (4)$$

For these elements we use $\sigma_s(\lambda) = 4 \times 10^{-17} \text{ cm}^2$ (McGuire 1968; Chapman and Henry 1971), $\lambda_{th}(S) = 1190 \text{ \AA}$ and $\sigma_{si}(\lambda) \approx 2 \times 10^{-17} \text{ cm}^2$ (McGuire 1968; Chapman and Henry 1972), and $\lambda_{th}(Si) = 1520 \text{ \AA}$.

The shielding problem is more complicated than the procedure adopted here, since silicon completely shields sulfur and carbon, sulfur completely shields carbon, they can all shield other photodestruction processes (e.g., photodissociation of CO or photo-ionization of CH), and they all partially shield each other. Furthermore, there are variations in the cross sections and the radiation field with λ which should be included in a detailed treatment. In this work we do

TABLE 4
CLOUD PARAMETERS FOR THE STANDARD RUN

<i>Physical parameters:</i>
$T = 20 \text{ K}$
$\zeta_p = 10^{-17} \text{ s}^{-1}$
<i>Reaction rates:</i>
$k_{26} = 1 \times 10^{-18} \text{ cm}^3 \text{ s}^{-1}$ ($C^+ - H_2$ radiative association)
<i>Abundances:</i>
$\xi_C = 7 \times 10^{-5}$
$\xi_O = 2 \times 10^{-4}$
$\xi_{He} = 1/12$
$\xi_S = 1.2 \times 10^{-5}$
$\xi_{Si} = 1.5 \times 10^{-6}$
$\xi_{Mg} = 1.5 \times 10^{-6}$
$\xi_{Fe} = 3 \times 10^{-7}$

not deal with the radiation transfer problem in all its complexity, but instead have chosen to introduce the most important characteristic attenuation lengths, photoionization rates, and self-shielding mechanisms.

III. RESULTS

In § II and Appendices A and B we have given the basic elements and equations necessary to determine the steady-state CO abundance in interstellar clouds due to binary gas phase reactions. In what follows we will discuss the solution of the abundance equations—in particular, the variation of CO with extinction of the ultraviolet radiation field for a variety of cloud temperatures and densities—and the dependence of these results on various cloud parameters. The results in this paper are restricted to regions where the fractional abundance of H_2 is large, column density to the center $N \gtrsim 6 \times 10^{20} \text{ cm}^{-2}$, and $n > 100 \text{ cm}^{-3}$.

From equation (1) it is possible to understand qualitatively the abundance of CO in relation to the three basic ion reactions which initiate molecule production, and where each ion is important. First, we discuss CO production in the region where C^+ remains at least partially ionized by the ultraviolet radiation field. The ratio of CO production by $H^+ + O$ charge exchange (the OH family) to radiative association of C^+ with H_2 (the CH-C₂ family) is approximately,

$$y_{CO} \approx \frac{k'x(C^+)x_M(O)}{a'x(O)[x_M(C) + x_M(C_2)]}, \quad (5)$$

where the small contribution from $x(H_3^+)$ can be neglected in this region. Using the following results from Appendix A,

$$\begin{aligned} x_M(O) &\approx k_5x(H^+)x(O)/[g_d(OH) + k'x(C^+)], \\ x(H^+) &\approx 10^{-1}(\zeta_p/n)\{\alpha x_e + k_5x(O) \\ &\quad + k'[x_M(O) + x_M(C)]\}^{-1} \\ &\quad (\text{for } f \gtrsim 0.9), \end{aligned}$$

and

$$\begin{aligned} x_M(C) + x_M(C_2) \\ \approx 0.5/fk_{26}x(C^+)\Gamma_{C^+}/[g_d(C_2) + a'x(O)], \quad (6) \end{aligned}$$

where $\Gamma_{C^+} = k'x(C^+)/[g_d(CH) + g''(C_2H)k'x(C^+)]$, we can approximate y_{CO} as

$$y_{CO} \approx \frac{2 \times 10^{-10}}{k_{26}\Gamma_0} \times \frac{(\zeta_p/n)e^{-232/T}[x(O)/x(C^+)]}{[\alpha x_e + k_5 x(O) + k'[x_M(O) + x_M(C)]]} , \quad (7)$$

where $\Gamma_0 = ax(O)/[g_d(C_2) + a'x(O)]$. When $T = 80$ K, and setting $\zeta_p \approx 10^{-17} s^{-1}$, $\xi_0 \approx 2 \times 10^{-4}$, $\xi_c \approx 7 \times 10^{-5}$, and $k_{26} = 10^{-16} \text{ cm}^3 \text{ s}^{-1}$, $y_{CO} \approx 10^3/n$, so that radiative association is not as important as $H^+ + O$ charge exchange for CO production when $n \lesssim 10^3 \text{ cm}^{-3}$. If k_{26} has a larger value $\gtrsim 10^{-15} \text{ cm}^3 \text{ s}^{-1}$, the $H^+ + O$ charge exchange chemistry can be neglected for CO production, except in regions of smaller $f = 2n(H_2)/n$ where the effective cosmic-ray ionization rate $\zeta_H \approx \zeta_p$. The ratio y_{CO} is a strongly decreasing function of temperature when $k_5 x(O) < \alpha x_e$, which occurs for $T \approx 30\text{--}40$ K. Consequently, the C^+ radiative association becomes more important as the temperature decreases, and when $T \lesssim 30$ K it dominates CO production for $n > 10^2 \text{ cm}^{-3}$.

The above discussion of temperature suggests that, at low temperatures ($T \lesssim 30$ K), in the transition region $x(CO)$ is given approximately by

$$x(CO) \approx \frac{0.5k_{26}\Gamma_0\Gamma_{C^+}x(C^+)}{g(CO) + k_{25}x(He^+)} , \quad (8)$$

where the small contribution from $x(H_3^+)$ can be neglected. We can show from equation (8), the approximate conservation condition $\xi_c \approx x(CO) + x(C^+) + x(C I)$, and simplified forms of equations (A1) and (A5) that C^+ will undergo a transition to CO and C I at a characteristic optical depth $\tau_v (N/2 \times 10^{21} \text{ cm}^{-2}) \approx 1\text{--}2$. The relative abundance of CO and C I will depend on k_{26} and n . It can also be shown in this model that for increasing optical depth, $\tau_v \gtrsim 2\text{--}3$, $x(CO)$ decreases, eventually going to zero at large optical depth. This result is a consequence of neglecting reactions with neutral carbon which bring it into molecular form. In this work these are the ion-molecule reactions of H_3^+ ; however, grains may also be important in these regions (see Watson and Salpeter 1972 and Allen and Robinson 1975 for a discussion of molecule formation on grains).

Deep in a cloud, where the ultraviolet radiation field which ionizes carbon and dissociates CO is attenuated, the CO abundance (at low temperatures) is determined by $x(H_3^+)$ and $x(He^+)$. We can estimate $x(CO)$ in the steady state by approximating the fractional abundance of carbon, $\xi_c \approx x(C^+) + x(CO) + x(C)$, and using equations (A1)–(A5) and (A7) in equation (1),

$$x(CO) \approx \frac{x(H_3^+)\xi_c}{x(H_3^+) + \delta x(He^+)} , \quad (9)$$

where $\delta \approx 0.75\alpha x_e/[\alpha x_e + 0.5k_{26} + k'x_M(O)]$. Thus $x(CO) \approx \xi_c$ when $x(H_3^+)/x(He^+) \approx O(1)$, which requires (from eqs. [A5] and [A7]) that $x_e \approx 5 \times 10^{-6}$; otherwise there will be incomplete conversion to CO even in dark clouds. Because the C^+ recombines to form CO and C I, and the CO and C I are destroyed by He^+ and H_3^+ , respectively, there can be significant C I if the H_3^+ abundance is too low. The major difficulty with the results for this regime is the long time scale required for equilibration in the ion-molecule scheme, $t \gtrsim 3 \times 10^6$ yr (Langer and Glassgold 1976) which is comparable with various dynamical times. Oppenheimer and Dalgarno (1975) have noted similar problems with the radiative association chemistry at large optical depths. We note again that grains may be important in this context or, as suggested by the work of Glassgold and Langer (1976a) on thermal-chemical instabilities in CO clouds, the CO abundance in these regions may be a consequence of cloud evolution.

To understand where the Herbst and Klemperer (1973) picture of molecule production holds—that is, $x(CO) \approx \xi_c$ (at least within the context of steady-state calculations)—it is necessary to determine where $x_e \lesssim 5 \times 10^{-6}$. The electron density, in regions where $g(C)$ and $g(CO)$ are attenuated, is determined by $x(H^+)$, $x(S^+)$, $x(Si^+)$, and $x(Mg^+)$, the sum of which must be $\lesssim 3 \times 10^{-6}$ for $x(CO) \approx \xi_c$. Now $x(H^+) \lesssim 2 \times 10^{14}\zeta_p/n$ [using $x_e \approx 5 \times 10^{-6}$ and $x_M(O) + x_M(C) + x_M(C_2) \gtrsim 10^{-7}$] so that $x(H^+) < 2 \times 10^{-6}$ if n exceeds a critical density, $n_{cr} \approx 2 \times 10^8 (\zeta_p/10^{-17})$. Similarly, $x(S^+) \lesssim 3 \times 10^{-6}$ when $g(S) \lesssim 0.4\alpha x_e$ (using $\xi_S \approx 10^{-5}$). If we set $x_e \approx 5 \times 10^{-6}$, $T \approx 10\text{--}20$ K, and $G_0(S) \approx 9 \times 10^{-10} \text{ s}^{-1}$ (de Boer, Koppenaal, and Pottasch 1973), there is a critical distance into a cloud, N_{cr} , beyond which $x(S^+) \lesssim 3 \times 10^{-6}$. Neglecting self-shielding effects, we find $N_{cr} \gtrsim 10^{21} \ln(2 \times 10^7/n)$. These restrictions on n and N indicate that the steady-state Herbst and Klemperer (1973) model is applicable to $n \gtrsim 10^3 \text{ cm}^{-3}$ and a total column density $N \gtrsim 2 \times 10^{22} \text{ cm}^{-2}$. When self-shielding and partial shielding by neutral carbon is included, this critical total column density is reduced somewhat to $\sim 1.5 \times 10^{22} \text{ cm}^{-2}$ (or $A_v \approx 7$ through a cloud).

In Figure 1 we plot $x(CO)$ as a function of optical depth into a cloud measured in terms of $\tau_v = N(2 \times 10^{21} \text{ cm}^{-2})^{-1}$ using a standard set of parameters. Unless otherwise stated, these are the following: (1) $\zeta_p = 10^{-17} \text{ s}^{-1}$, $k_{26} = 10^{-16} \text{ cm}^3 \text{ s}^{-1}$, $\xi_0 = 2 \times 10^{-4}$, $\xi_c = 7 \times 10^{-5}$, and $f \approx 1$ (see Table 4 for a list of these including minor constituents); (2) the mean optical depths for grain attenuation, $\tau_g(X)$, which are listed in Table 5; and (3) the ion-molecule and photodestruction processes listed in Tables 1–3, and Glassgold and Langer (1975, 1976b). The results are calculated for three values of the temperature, $T = 20, 40$, and 80 K, and for a range of densities $n(H_2) = 100\text{--}5000 \text{ cm}^{-3}$. There are a number of noteworthy features in these results which emphasize the physical picture of CO production that has already been presented.

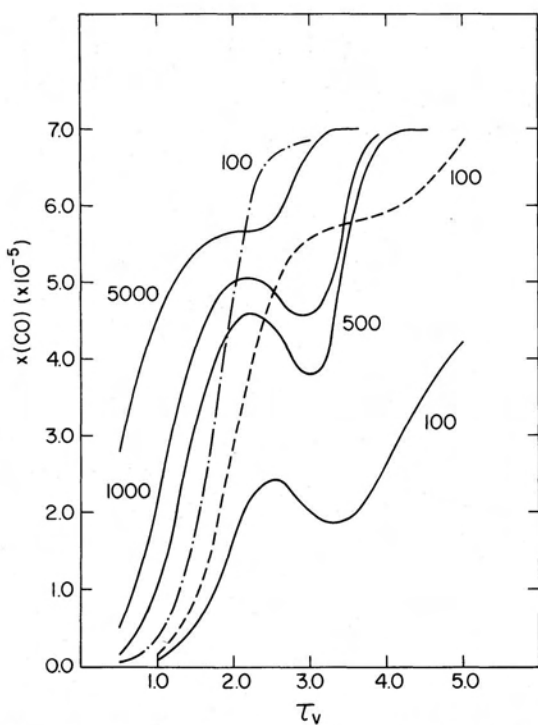


FIG. 1.—Fractional concentrations of CO relative to hydrogen, $x(\text{CO}) = n(\text{CO})/n$, as a function of optical depth into a cloud, $\tau_v = N(2 \times 10^{21} \text{ cm}^{-2})^{-1}$. Except as otherwise noted, the parameters are those listed in Table 4; each curve is labeled with $n(\text{H}_2)$. The solid curves are for $T = 20 \text{ K}$, while the dashed curve is $T = 40 \text{ K}$ and the dash-dot curve is $T = 80 \text{ K}$.

In general, as the temperature increases from 20 to 80 K, $x(\text{CO})$ increases and the transition region for $\text{C}^+ - \text{CO}$ conversion narrows. This increase is explained by the larger rate for $\text{H}^+ + \text{O}$ charge exchange [$k_5 = 10^{-9} \exp(-232/T) \text{ cm}^3 \text{ s}^{-1}$] with increasing T . These results are in accord with the discussion on the relative importance of C^+ radiative association and $\text{H}^+ + \text{O}$ charge exchange for CO production. The

fractional abundance $x(\text{CO})$ is sensitive to temperature for $T \gtrsim 30 \text{ K}$ and $n \lesssim 10^3 \text{ cm}^{-3}$.

At fixed temperature an increase in density results in $x(\text{CO})$ increasing, because (1) at small optical depths the photodestruction reaction rates decrease with density, $g(X) = G(X)/n$ and (2) at large optical depths $n(\text{He}^+)$ decreases and $n(\text{H}_3^+)$ increases with increasing n (see eqs. [9], [A5], and [A7]). In accord with our previous discussion of the relative importance of H_3^+ and He^+ for $x(\text{CO})$ at large optical depths, there is considerable neutral carbon present when $n(\text{H}_2) \lesssim 10^3 \text{ cm}^{-3}$ at low temperatures.

Under all temperature and density conditions $x(\text{CO})$ increases, beginning at $\tau_v = 0.5$, with increasing extinction into a cloud. As the ultraviolet radiation field is attenuated from the outside of a cloud, the molecular photodestruction rates decrease and $x(\text{CO})$ increases. There is, however, a pronounced decrease or leveling off in $x(\text{CO})$ (at low temperatures) when $\tau_v \approx 2-3$ because of a smaller, decreasing CO production rate and a relatively constant destruction rate (due primarily to He^+ dissociative charge exchange). The decreased production is due to attenuation of $G(\text{C})$ and the consequent decrease in $x(\text{C}^+)$. These numerical results agree with the discussion in § II of the carbon monoxide abundance predicted by equation (8), so that if $x(\text{H}_3^+) \ll x(\text{He}^+)$, C^+ will recombine to C I when $g(\text{C}) \lesssim 0.1\alpha x_e$. As discussed previously, the H_3^+ molecule production mechanism will not dominate until larger values of $\tau_v \approx 3-4$, and for $\tau_v \gtrsim 3$, $x(\text{CO})$ increases again.

There are different transition regions for the CO abundance corresponding to the characteristic regions for attenuation of the ultraviolet radiation field leading to (1) photodestruction of molecules, $\tau_v \lesssim 2$; (2) ionization of carbon; and (3) ionization of sulfur and the heavy metals. It should be noted, however, that if molecule production by grains, with a characteristic rate $\sim 10^{-17}-10^{-16} \text{ cm}^3 \text{ s}^{-1}$, is included then the decrease in $x(\text{CO})$ for $\tau_v \approx 2-3$ is smaller. The effects of various parameter changes on $x(\text{CO})$ and the different transition regions is discussed below.

In Figure 2 we indicate the effect on $x(\text{CO})$ of increasing the radiative association rate, k_{26} , to $10^{-15} \text{ cm}^3 \text{ s}^{-1}$ for a range of densities $n(\text{H}_2)$ (here $T = 20 \text{ K}$ and the remaining parameters are given in Table 4). Where radiative association is the dominant production mechanism ($\tau_v \lesssim 3$), $x(\text{CO})$ increases with increasing k_{26} . The increase is nearly linear at very small optical depths where $x(\text{CO}) \ll x(\text{C}^+)$, but becomes nonlinear in the transition region where $x(\text{CO}) \approx x(\text{C}^+)$. Increasing k_{26} by a factor of 10 only increases $x(\text{CO})$ by ~ 2 , and it is not likely that abundance measurements in thicker clouds could be used to estimate this rate.

In Figure 3 the density is fixed at $n(\text{H}_2) = 500 \text{ cm}^{-3}$ and $T = 20 \text{ K}$, and we consider the effect of varying other uncertain rates and parameters. The solid line reproduces the $x(\text{CO})$ curve from Figure 1, and the four dashed curves are labeled with the single parameter which is changed.

The value of ζ_p in diffuse clouds has been estimated

TABLE 5
MEAN GRAIN ABSORPTION FOR ULTRAVIOLET*

Species	$\tau_o(X) = N/N_o(X):$ $N_g (\text{cm}^{-2})$
I. Ionization:	
OH.....	7×10^{20}
C, H ₂ O, C ₂	8×10^{20}
CH.....	9×10^{20}
S, CH ₂ , CH ₃	1×10^{21}
Fe, Mg, Si.....	1.2×10^{21}
II. Dissociative:	
CO, OH, C ₂	8×10^{20}
CH, CH ₂ , H ₂ O, C ₂ H.....	1.3×10^{21}

* Based on the average extinction curve of Bless and Savage 1972, extended by the OAO-3 measurements (York *et al.* 1973), and using an albedo of $\frac{1}{2}$ (see Glassgold and Langer 1974).

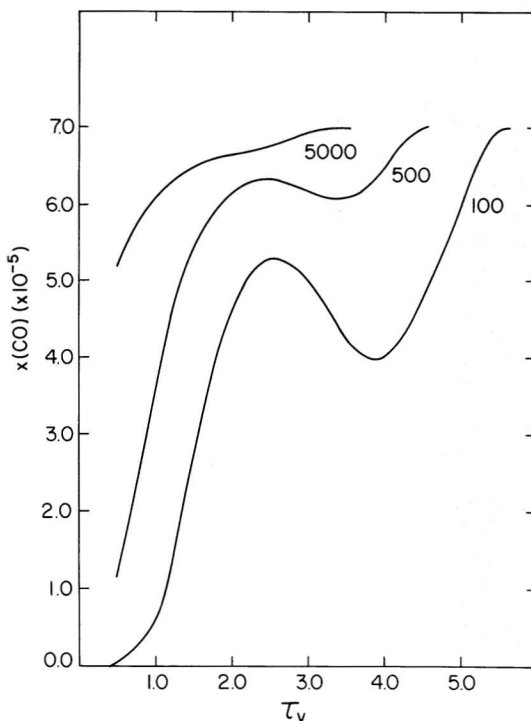


FIG. 2.—Fractional concentrations of CO relative to hydrogen, $x(\text{CO}) = n(\text{CO})/n$, as a function of optical depth into a cloud, $\tau_v = N(2 \times 10^{21} \text{ cm}^{-2})^{-1}$. The parameters are those listed in Table 4 except that a larger radiative association rate, $k_{28} = 10^{-15} \text{ cm}^3 \text{ s}^{-1}$ is used. Each curve is labeled with $n(\text{H}_2)$.

to lie in the range 10^{-17} – $5 \times 10^{-17} \text{ s}^{-1}$ (Black and Dalgarno 1973c; Jura 1974; O'Donnell and Watson 1974; Glassgold and Langer 1976b), while Spitzer and Tomasko (1968) estimate that $\zeta_p = 6 \times 10^{-18} \text{ s}^{-1}$ for cosmic rays with energies $\geq 100 \text{ MeV}$. We take the view that the increased values of ζ_p estimated for diffuse clouds arise from a spectrum of cosmic rays with energies less than 100 MeV. The characteristic stopping distance for 2 MeV protons is a column density, $N \approx 10^{21} \text{ cm}^{-2}$. With increasing energy, $N \propto E^2/\ln(E)$, so that cosmic rays with energies $E > 10 \text{ MeV}$ will penetrate the regime which is under consideration in this work. Increasing ζ_p to $5 \times 10^{-17} \text{ s}^{-1}$ in Figure 3 yields results in accord with the earlier discussions on H_3^+ , He^+ , and CO. At small optical depths there is little change because the primary destruction of CO is by photodissociation. With increasing τ_v , however, $x(\text{CO})$ is smaller than the standard run because destruction by He^+ is larger [$x(\text{He}^+) \propto \zeta_p$].

There is considerable uncertainty in the CO photo-dissociation rate (Solomon and Klemperer 1972), and for comparison we consider the lower value of the range suggested by Glassgold and Langer (1976b), $G_0(\text{CO}) = 3 \times 10^{-12} \text{ s}^{-1}$. At small $\tau_v \lesssim 2$, where photodestruction dominates, $x(\text{CO})$ increases, eventually

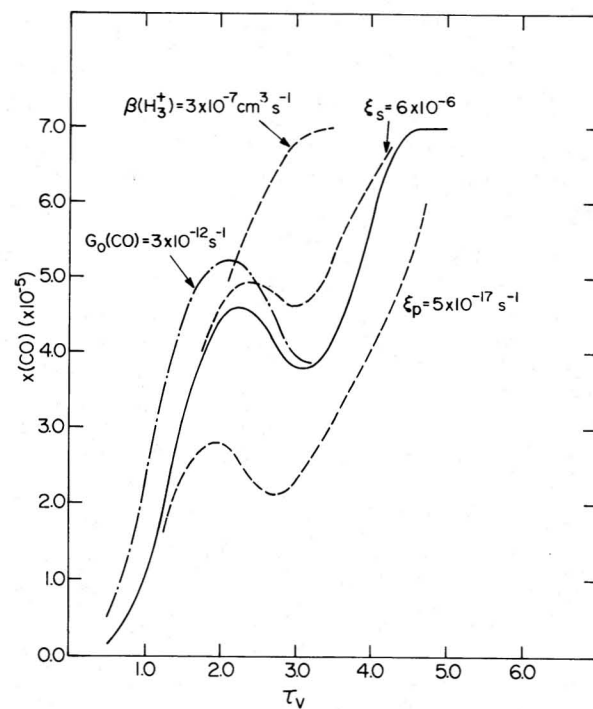


FIG. 3.—Fractional concentrations of CO relative to hydrogen, $x(\text{CO}) = n(\text{CO})/n$, as a function of optical depth into a cloud, $\tau_v = N(2 \times 10^{21} \text{ cm}^{-2})^{-1}$. The density is fixed at $n(\text{H}_2) = 500 \text{ cm}^{-3}$ and the solid curve is based on the parameters listed in Table 4. Each of the dashed curves changes only one parameter or rate and these changes are the following: $\zeta_p = 5 \times 10^{-17} \text{ s}^{-1}$, $G_0(\text{CO}) = 3 \times 10^{-12} \text{ s}^{-1}$, $\xi_s = 6 \times 10^{-6}$, and $\beta(\text{H}_3^+) = 3 \times 10^{-7} \text{ cm}^3 \text{ s}^{-1}$.

ally merging with the standard curve at the point where He^+ dissociative charge exchange is the dominant source of destruction.

In Figure 3 we plot the results for $\xi_s = 6 \times 10^{-6}$, half the value in the standard run. Varying the abundance of sulfur does not change significantly the transition point where H_3^+ dominates CO production. Here we see the effect of the reduced self-shielding: the sulfur remains ionized to greater depths compensating the smaller abundance of available sulfur. Because $x(\text{S}^+)$ is not changed much, x_e and $x(\text{H}_3^+)$ are unchanged. Increasing ξ_s to 1.4×10^{-4} generally doubles $x(\text{CO})$ but does not change the transition points; again various competing effects cancel. These results are not shown in Figure 3.

Finally, we consider the effect of fixing the dissociative recombination rate for H_3^+ at $\beta(\text{H}_3^+) = 3 \times 10^{-7} \text{ cm}^3 \text{ s}^{-1}$ (corresponding to the measurements of Leu, Biondi, and Johnsen 1973 at $T = 200 \text{ K}$), rather than using the temperature-dependent rate (Herbst and Klemperer 1973; Glassgold and Langer 1976b). Because $x(\text{H}_3^+) \propto 1/\beta(\text{H}_3^+)$ (eq. [A7]), the H_3^+ is much larger for a given value of x_e , and the transition to the H_3^+ regime occurs for smaller τ_v . Furthermore, the decreasing features of $x(\text{CO})$ are no longer present. We should emphasize again that this feature

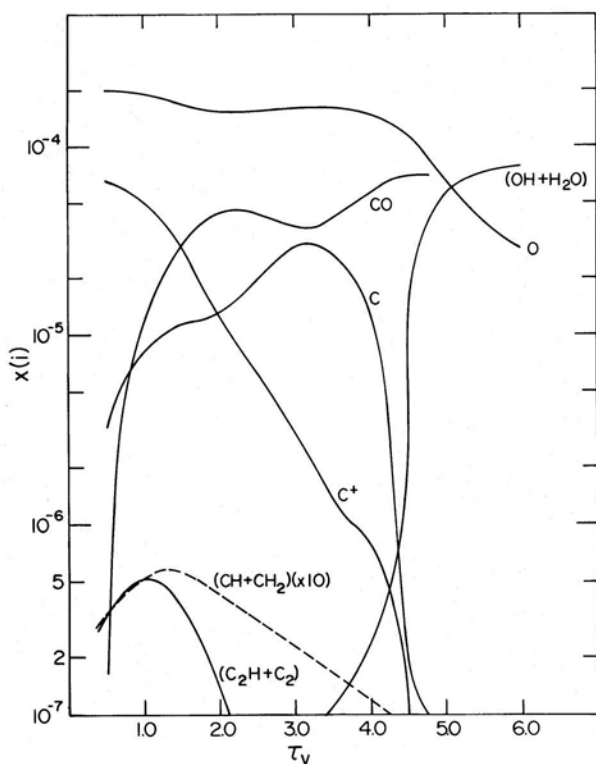


FIG. 4.—Fractional concentrations, $x(X_i) = n(X_i)/n$, of the major carbon- and oxygen-bearing species as a function of optical depth into a cloud, $\tau_v = N(2 \times 10^{21} \text{ cm}^{-2})^{-1}$. The parameters are those listed in Table 4, and the density is fixed at $n(\text{H}_2) = 500 \text{ cm}^{-3}$.

may be a spurious result because of all the uncertainties in parameters. For example, the grain attenuation of the ultraviolet radiation field may be roughly constant over a wide range of wavelengths due to different values of the albedo at short wavelengths (Witt and Lillie 1973). In this case a calculation using $\tau_g(X) = N/10^{21} \text{ cm}^{-2}$ shows that $x(\text{CO})$ levels off at $\tau_v \approx 3-4$ [for $n(\text{H}_2) = 500 \text{ cm}^{-3}$] but does not decrease. Because all the attenuation lengths are the same the H_3^+ mechanism is becoming important in the region where $g(\text{C})$ is getting small and carbon is not being ionized.

In Figures 4 and 5 the fractional abundances of the major neutral and ionic species are plotted as a function of τ_v for the standard parameters, $n = 10^3 \text{ cm}^{-3}$ [$n(\text{H}_2) = 500 \text{ cm}^{-3}$], and $T = 20 \text{ K}$. The behavior of most of the species plotted in these figures can be understood from the equations in Appendices A and B, the previous discussion of the characteristic attenuation lengths, and the three molecule initiating mechanisms. The abundances for $\tau_v \geq 4-4.5$ may not be correct because of the long time needed to reach steady state in the H_3^+ regime (Langer and Glassgold 1976). These curves are exemplary of the abundance variations with optical depth; other values of the density give similar results though the characteristic changes occur at different values of τ_v .

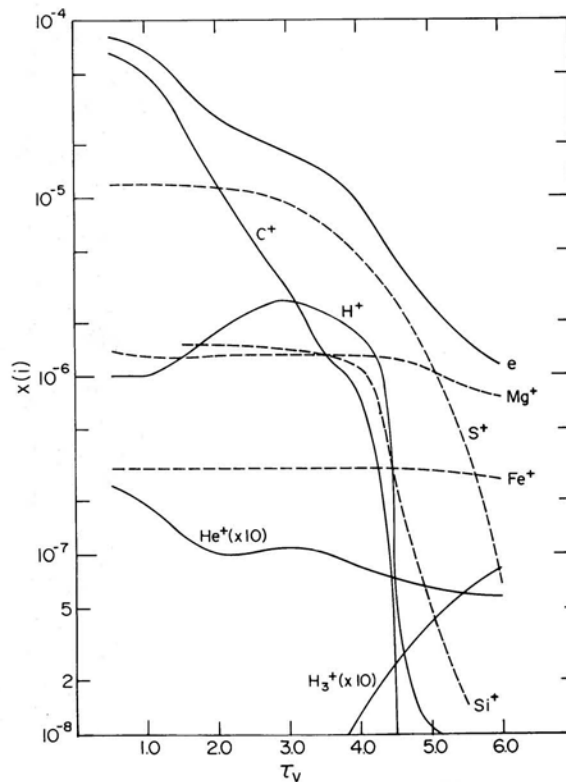


FIG. 5.—Fractional abundances of the major ions and the electrons for the atomic and molecular abundances in Fig. 4.

IV. CONCLUSION

The theory for molecule production presented here is valid for essentially all interstellar cloud conditions under assumptions of steady state, providing $n \geq 50 \text{ cm}^{-3}$, $\tau_v \geq 0.5$, and molecule formation on grains can be neglected. This work bridges the gap between diffuse and thick clouds and discusses the $\text{C}^+ - \text{CO}$ transition with attenuation in thick clouds. There are characteristic column densities for this transition for different cloud conditions (for warm clouds, $T \geq 40 \text{ K}$; see also Glassgold and Langer 1975).

The inclusion of C_2H , C_2 , sulfur, and the metal ions in this work leads to a number of differences with previous calculations. In comparison with Oppenheimer and Dalgarno (1975) these differences are primarily due to the role of C_2H and C_2 production of CO, which can significantly enhance CO production. For the Herbst and Klempner (1973) results these differences are primarily due to the contribution of the heavy metals to the electron abundance and the inclusion of $\text{C}^+ + \text{H}_2$ radiative association.

When the column density to the center $N \geq (2-4) \times 10^{21} \text{ cm}^{-2}$ ($\tau_v \geq 1-2$), significant amounts of the available carbon will be in the form of CO. At the temperatures characteristic of many molecular clouds ($T \leq 20 \text{ K}$), however, there can also be significant amounts of C I. To compare the calculations in this paper with observations we have integrated $x(\text{CO})$ to obtain total column densities, $N(\text{CO})$, of CO through a cloud. In

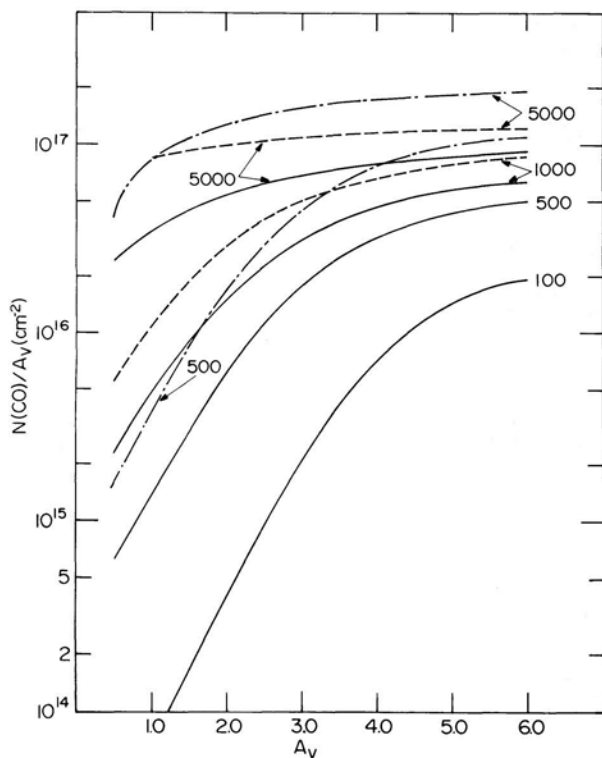


FIG. 6.—The integrated column densities of CO divided by the extinction, $N(\text{CO})/A_v$, as a function of extinction through a cloud [$A_v = N(2 \times 10^{21} \text{ cm}^{-2})^{-1}$]. The solid curves are for the parameters listed in Table 4; the dashed curves use a larger radiative association rate, $k_{26} = 10^{-15} \text{ cm}^3 \text{ s}^{-1}$; and the dash-dot curves use a larger fractional abundance of carbon, $\xi_c = 1.4 \times 10^{-4}$. The density $n(\text{H}_2)$ which labels each curve is assumed constant throughout the cloud.

these cloud models the density and temperature are kept fixed.

In Figure 6 we plot $N(\text{CO})/A_v$ versus the total extinction through a cloud, $A_v = N(2 \times 10^{21} \text{ cm}^{-2})^{-1}$, for a range of molecular hydrogen densities, $n(\text{H}_2) = 100\text{--}5000 \text{ cm}^{-3}$. The solid lines are for the standard parameters listed in Table 4; the dashed curves give the results when the radiative association rate for $\text{C}^+ + \text{H}_2$ is increased to $k_{26} = 10^{-15} \text{ cm}^3 \text{ s}^{-1}$; and the dash-dot curves consider increasing the available carbon to $\xi_c = 1.4 \times 10^{-4}$. Encenaz, Falgarone, and Lucas (1975) have mapped in detail the ρ Ophiuchi dark cloud in the $J = 1 \rightarrow 0$ line of both $^{12}\text{C}^{16}\text{O}$ and $^{13}\text{C}^{16}\text{O}$. Column densities of CO were derived and compared with visual extinction measurements using

star counts. For $A_v > 2$, $N(\text{CO})/A_v \approx 10^{17} \text{ cm}^{-2} \text{ mag}^{-1}$ corresponding to a mean fractional abundance of CO, $x(\text{CO}) = N(\text{CO})/N = 5 \times 10^{-5}$. This result is consistent with the curves plotted in Figure 6 for a variety of parameters and suggests that $n(\text{H}_2) \approx 10^3\text{--}5 \times 10^3$, $\xi_c \approx 10^{-4}$, and $k_{26} \approx 10^{-16}\text{--}10^{-15} \text{ cm}^3 \text{ s}^{-1}$ are appropriate. When $A_v > 4.5$ there is some scatter in the data, some points cluster at $N(\text{CO})/A_v \approx (1.5\text{--}2.0) \times 10^{17} \text{ cm}^{-2} \text{ mag}^{-1}$, while others cluster at $N(\text{CO})/A_v \approx 8 \times 10^{16} \text{ cm}^{-2} \text{ mag}^{-1}$. Observational uncertainties and the interpretation of $N(\text{CO})$ and A_v from the data probably yield factor of 2 uncertainties in these values (Encenaz 1975). The larger values of $N(\text{CO})/A_v$ (disregarding the uncertainties) can best be explained by $\xi_c \approx (1.0\text{--}1.4) \times 10^{-4}$ and $n(\text{H}_2) \approx 5000 \text{ cm}^{-3}$, while the lower values might be appropriate to regions with $n(\text{H}_2) \approx 1000 \text{ cm}^{-3}$. At small A_v , $2 \geq A_v \geq 1$, values for $N(\text{CO})/A_v \approx (4\text{--}5) \times 10^{15}$ and are consistent with the curves in Figure 6 for $n(\text{H}_2) \approx 500\text{--}1000 \text{ cm}^{-3}$. The difference in $N(\text{CO})/A_v$ for small and large extinction is best understood in terms of the density. Inhomogeneities in density probably exist in the cloud structure with $n(\text{H}_2)$ increasing going toward the center. The measurements at small A_v are at the outside of the cloud, and our interpretation of lower densities is consistent with the inhomogeneous picture of clouds. Finally, Dickman (1975) has surveyed a number of dark clouds in CO and finds similar results for $A_v \geq 2$, in agreement with the curves in Figure 6.

The grain formation mechanisms of Watson and Salpeter (1972) and Allen and Robinson (1975) can contribute to the production rate of the simple oxygen- and carbon-bearing molecules discussed in this paper, and it may be the main source of some other molecules (e.g., CH_4 , CH_3). Details of its role depend on the formation rate, estimated to lie in the range $10^{-17}\text{--}10^{-16} \text{ cm}^3 \text{ s}^{-1}$ (Watson 1972b), which is a function of grain size, molecule ejection mechanisms, and the grain charge. The extent of its role compared with gas phase reactions depends on many other factors, such as n , T , ζ_p , and the radiative association rate for C^+ (the uncertainty in this rate is probably the most significant of any used in this work). Within the context of the calculations in this paper gas phase reactions are likely to be more important than grains for producing molecules, though grains possibly contribute to $x(\text{CO})$, through the CH_x and OH_x family, for $\tau_v \geq 4$.

The author would like to thank Drs. A. E. Glassgold, S. Green, and R. Dickman for useful conversations. The author is grateful for support as an NRC-NAS Senior Research Associate during the completion of this work.

APPENDIX A

The balance equation for the fractional abundance of C^+ is

$$x(\text{C}^+) = \frac{g(\text{C})x(\text{C}) + k_{25}x(\text{He}^+)x(\text{CO})}{\alpha x_e + 0.5fk_{26} + k'[x_M(\text{O}) + x_M(\text{C})]}, \quad (\text{A1})$$

where $x_M(O) = x(OH) + x(H_2O) + x(O_2)$ and $x_M(C) = x(CH) + x(CH_2)$. The destruction mechanisms in the denominator are radiative recombination ($\alpha \approx 1.9 \times 10^{-10} T^{-0.7} \text{ cm}^3 \text{ s}^{-1}$), radiative association with H_2 , and ion-molecule reactions with OH, H_2O , and O_2 ($k' \approx k_{17} + k_{18} \approx k_{19} + k_{20} \approx k_{32} + k_{33} \approx 2 \times 10^{-9} \text{ cm}^3 \text{ s}^{-1}$, in the notation of Glassgold and Langer 1976b) and CH and CH_2 ($k' = k_{29} = k_{35} \approx 2 \times 10^{-9} \text{ cm}^3 \text{ s}^{-1}$). The production terms in the numerator are photoionization [rate constant $g(C) \equiv G(C)/n$, where the ionization rate $G(C) = \int_{912}^{1100} \sigma(\lambda)I(\lambda)d\lambda$] and dissociative charge exchange of He^+ with CO ($k_{25} = 1.6 \times 10^{-9} \text{ cm}^3 \text{ s}^{-1}$).

The remaining equations for the carbon- and oxygen-bearing molecules (excluding CO which is discussed in the text) are given below and result from a number of simplifications and approximations in which the low abundance constituents are eliminated:

$$x_M(O) \approx \frac{[k_5 x(H^+) + K x(H_3^+)]x(O)}{g_d(OH) + k' x(C^+) + k_{56} x(He^+)}, \quad (A2)$$

$$x_M(C) \approx \frac{0.5f k_{26} x(C^+) + K x(H_3^+)x(C)}{g_d(CH) + k_{29} x(C^+)g''(C_2H) + a_4 x(O) + k_{48} x(He^+)}, \quad (A3)$$

$$g''(C_2H) = \frac{g'(C_2H)}{g'(C_2H) + a_7 x(O)}, \quad g'(C_2H) = g(C_2H) \frac{g_d(C_2) + a_7 x(O)}{g(C_2) + a_7 x(O)},$$

$$x_M(C_2) = \frac{k_{29} x_M(C)x(C^+)}{g_d(C_2) + k_{48} x(He^+) + a_7 x(O)}, \quad (A4)$$

where $x_M(C_2) = x(C_2) + x(C_2H)$ and $K = 3 \times 10^{-9} \text{ cm}^3 \text{ s}^{-1}$. The essence of these results is that ionization and charge exchange recycle OH, H_2O , etc., back into OH, H_2O , etc. (Glassgold and Langer 1975). Equation (A2) must be modified when $x(C^+)/x(O) \lesssim 10^{-2}$ and $x(C^+)/[x(H^+) + x(He^+)] \lesssim 1$ because there may be significant abundance of O_2 (produced by $O + OH \rightarrow O_2 + H$). Only reactions which remove these molecules from the cycle (e.g., $\gamma + CH \rightarrow C + H$, $C^+ + CH_2 \rightarrow C_2H^+ + H$, or $CH_2 + O \rightarrow CH + CO$) need be considered as destruction mechanisms, providing we can consider only the total neutral molecule abundance in the cycle [i.e., $x_M(C) = x(CH) + x(CH_2)$]. Furthermore, the sums $x_M(O)$ and $x_M(C)$ have the advantage of reducing the dependence on the uncertain branching ratios for dissociative recombination [e.g., $\beta_8(CH_3^+)$].

The important role of C_2 and C_2H in the CO abundance calculations does not seem to have been properly emphasized before. The major exit channels competing with photodissociation of CH and CH_2 are the ion-molecule reactions with C^+ . These reactions are more important than CO production by neutral molecule reactions if $x(C^+)/x(O) \gtrsim 10^{-2}$, a condition essentially valid throughout most of the transition region. The C_2H which is produced from the reactions $C^+ + (CH \text{ and } CH_2)$ can be photodissociated to produce C_2 , $\gamma + C_2H \rightarrow C_2 + H$. Both C_2H and C_2 form CO through neutral molecule reactions with O. The only other significant exit channel is photodissociation of C_2 , $\gamma + C_2 \rightarrow C + C$, with a probable rate $G_d(C_2) \approx 10^{-11} \text{ s}^{-1}$ (see the discussion by Solomon and Klempner 1972). The photoionization rate of C_2 , $G_i(C_2) \approx 10^{-10} \text{ s}^{-1}$, for Jura's (1974) ultraviolet radiation field, is estimated using a cross section of 10^{-17} cm^2 and an ionization potential of 12 eV. Throughout the transition region photodestruction primarily converts C_2 back to C_2H , because $G_i(C_2) > G_d(C_2)$ and the ultraviolet radiation which photoionizes and dissociates is in the same energy range and attenuates with the same characteristic optical depth. The small net photodestruction rate for removing molecules from the C_2H and C_2 cycle enhances the CO production rate.

The ions of hydrogen and helium are given by the following generalizations of the results of Glassgold and Langer (1976b):

$$x(He^+) = \frac{\xi_{He}\zeta(He)/n}{0.5fk_9 + k_{25}x(CO) + k[x_M(C) + x_M(C_2) + x_M(O)]}, \quad (A5)$$

where ξ_{He} is the abundance and $\zeta(He)$ the cosmic-ray ionization rate of helium. The destruction is by dissociative charge exchange with H_2 , $k_9 \approx 10^{-18} \text{ cm}^3 \text{ s}^{-1}$ and CO, $k_{25} = 1.6 \times 10^{-9} \text{ cm}^3 \text{ s}^{-1}$, and charge exchange and dissociative charge exchange with the remaining carbon- and oxygen-bearing molecules ($k \approx k_{48} \approx k_{21} \approx k_{22} \approx 5 \times 10^{-10} \text{ cm}^3 \text{ s}^{-1}$). Similarly the H^+ abundance is given by

$$x(H^+) = \frac{\zeta_H/n + 0.5fk_9x(He^+) + k_{18}x(C^+)[x(OH) + x(H_2O)]}{\alpha x_e + k_5 x(O) + k_{10} x_M(O) + k_{40}[x_M(C) + x_M(C_2)]}, \quad (A6)$$

where ζ_H is an effective cosmic-ray ionization rate for hydrogen in $H-H_2$ mixtures (Glassgold and Langer 1976b). Finally,

$$x(H_3^+) = \frac{0.5f\xi_2(H_2^+)/n}{\beta(H_3^+)x_e + k'\xi_0}. \quad (A7)$$

The destruction of H_3^+ is dominated by dissociative recombination for $x_e \gtrsim 5 \times 10^{-7}$ [$\beta_1(H_3^+) \approx 4 \times 10^{-6}/T^{0.5} \text{ cm}^3 \text{ s}^{-1}$] and when $x_e \lesssim 5 \times 10^{-7}$ by ion-molecule reactions with oxygen and all the oxygen-bearing molecules with a mean rate $k' \approx 2 \times 10^{-9} \text{ cm}^3 \text{ s}^{-1}$. The reactions with carbon and the CH family can be neglected because $x_M(C) + x_M(C_2) + x(C) \ll \xi_0$ when $x_e < 10^{-6}$; similarly, charge exchange with sulfur and the heavy metal atoms can be neglected.

Balance equations for H_3O^+ , HCO^+ , and for the remaining low-abundance molecular and molecular-ion species can be derived from the reactions and rates in Tables 1–3 and Glassgold and Langer (1976b). Equations (A1)–(A4) must be supplemented by the approximate conservation equations for the constant gaseous fractions of oxygen and carbon, $\xi_0 \approx x(O) + x(CO) + x(H_2O) + x(OH) + 2x(O_2)$, and $\xi_C \approx x(C) + x(C^+) + x(CO) + x_M(C) + 2x_M(C_2)$. When it is necessary to calculate the abundance of individual species, such as OH or O_2 , estimates of branching ratios for dissociative recombination and photodissociation must be made. As discussed previously, these estimates do not change significantly the CO abundance, but do affect the abundance of the molecules, OH, O_2 , etc. (see Glassgold and Langer 1975, 1976b).

APPENDIX B

The chemistry of sulfur has been discussed by Oppenheimer and Dalgarno (1974a) who noted that it entered the molecular chain primarily through reactions of H_3^+ with neutral sulfur, because $S^+ + H_2 \rightarrow SH^+ + H$ is endothermic. The sulfur ion is neutralized by either radiative recombination with electrons or charge exchange with heavy metals (the few molecules with lower ionization potentials than sulfur are not abundant enough to contribute to neutralizing sulfur). By analogy with the data available for O^+ (Ferguson 1973), S^+ will charge exchange with Fe and Ca, but not Mg or Na. In the abundance calculations presented here we have used balance equations for S^+ and the major sulfur molecules, supplemented by the conservation condition for gaseous sulfur. The following equation, however, gives the behavior of $x(S^+)$ through the transition region,

$$x(S^+) \approx \frac{g(S)\xi_S}{\alpha x_e + k_{65}x(\text{Fe}) + g(S)}, \quad (\text{B1})$$

where $g(S) \equiv G(S)/n$ and $G(S)$ is the photoionization rate.

The metals, Mg and Fe, do not readily form molecules (Oppenheimer and Dalgarno 1974b) but, unlike sulfur, are ionized by charge exchange with $H_3^+[H_3^+ + (\text{Mg}, \text{Fe}) \rightarrow H_2 + H + (\text{Mg}^+, \text{Fe}^+)]$. Furthermore, other molecular ions, such as HCO^+ and O_2^+ , will charge exchange with these metals, as well as S^+ with Fe and Si^+ with Mg. These metals, which are a main source of ions in the interiors of dark, dense clouds, have an ion abundance

$$x(\text{Mg}^+) \approx \frac{\{g(\text{Mg}) + k_{65}[x(\text{Si}^+) + x(\text{Fe}^+)] + K_9 \sum_i x(i)\}\xi_{\text{Mg}}}{\alpha x_e + \{g(\text{Mg}) + k_{65}[x(\text{Si}^+) + x(\text{Fe}^+)] + K_9 \sum_i x(i)\}}, \quad (\text{B2})$$

$$x(\text{Fe}^+) \approx \frac{[g(\text{Fe}) + k_{66}x(S^+) + K_9 \sum_i x(i)]\xi_{\text{Fe}}}{\alpha x_e + k_{65}x(\text{Mg}) + [g(\text{Fe}) + k_{66}x(S^+) + K_9 \sum_i x(i)]}, \quad (\text{B3})$$

where $i = H_3^+, HCO^+, H_3O^+, O_2^+$, etc.

The silicon ion undergoes radiative association with H_2 (Oppenheimer and Dalgarno 1972b) and ion-molecule reactions with O_2 and OH. While we use the balance equations for silicon, its ions and molecules, in our calculations the behavior of Si^+ throughout the transition is given approximately by

$$x(\text{Si}^+) \approx \frac{[g(\text{Si}) + K_9 \sum_i x(i)]\xi_{\text{Si}}}{\alpha x_e + k_{65}x(\text{Mg}) + 0.5k_{57} + k_{58}[x(O_2) + x(OH)] + [g(\text{Si}) + K_9 \sum_i x(i)]}, \quad (\text{B4})$$

where i is the same as above. We neglect the metals, Al, Ca, Na, and Cl because of their small abundance compared with Mg, Fe, and Si (Morton *et al.* 1973). From the above discussion it is clear how they can be included.

REFERENCES

- Allen, M., and Robinson, G. W. 1975, *Ap. J.*, **195**, 81.
- Black, J. H., and Dalgarno, A. 1973a, *Ap. Letters*, **15**, 79.
- . 1973b, *Ap. J. (Letters)*, **184**, L10.
- . 1973c, *ibid.*, L101.
- Black, J. H., Dalgarno, A., and Oppenheimer, M. 1975, *Ap. J.*, **199**, 633.
- Bless, R. C., and Savage, B. D. 1972, *Ap. J.*, **171**, 293.
- Chapman, R. D., and Henry, R. J. W. 1971, *Ap. J.*, **168**, 169.
- . 1972, *Ap. J.*, **123**, 243.
- Dalgarno, A., and Oppenheimer, M. 1974, *Ap. J.*, **192**, 597.
- Dalgarno, A., Oppenheimer, M., and Berry, R. S. 1973, *Ap. J. (Letters)*, **183**, L21.
- Dalgarno, A., Oppenheimer, M., and Black, J. H. 1973, *Nature*, **245**, 100.
- Davis, D. D., Fisher, S., and Schiff, R. 1974, *J. Chem. Phys.*, **61**, 2213.
- de Boer, K. S., Koppenaal, K., and Pottasch, S. R. 1973, *Astr. and Ap.*, **28**, 145.

- Dickman, R. 1975, unpublished, Ph.D. Thesis, Columbia University.
- Encrenaz, P. J. 1975, private communication.
- Encrenaz, P. J., Falgarone, E., and Lucas, R. 1975, *Astr. and Ap.*, **44**, 73.
- Fehsenfeld, F. C., Dunkin, D. B., and Ferguson, E. E. 1974, *Ap. J.*, **188**, 43.
- Ferguson, E. E. 1973, *Atomic Data and Nuclear Data Tables*, **12**, 159.
- Field, G. B., and Steigman, G. 1971, *Ap. J.*, **166**, 59.
- Glassgold, A. E., and Langer, W. D. 1974, *Ap. J.*, **193**, 73.
- _____. 1975, *ibid.*, **197**, 347.
- _____. 1976a, *ibid.*, **204**, 403.
- _____. 1976b, *ibid.*, **206**, 85.
- Herbst, E. 1975, private communication.
- Herbst, E., and Klemperer, W. 1973, *Ap. J.*, **185**, 505.
- Jura, M. 1974, *Ap. J.*, **191**, 375.
- Kim, J. K., Theard, L. P., and Huntress, W. T. 1975, *J. Chem. Phys.*, **62**, 45.
- Langer, W. D., and Glassgold, A. E. 1976, *Astr. and Ap.*, in press.
- Leu, M. T., Biondi, M. A., and Johnsen, R. A. 1973, *Phys. Rev.*, **7A**, 292; **8A**, 420.
- McGuire, E. J. 1968, *Phys. Rev.*, **175**, 20.
- Morton, D. C. 1975, *Ap. J.*, **197**, 85.
- Morton, D. C., Drake, J. F., Jenkins, E. B., Rogerson, J. B., Spitzer, L., and York, D. G. 1973, *Ap. J. (Letters)*, **181**, L103.
- O'Donnell, E. J., and Watson, W. D. 1974, *Ap. J.*, **189**, 89.
- Oppenheimer, M., and Dalgarno, A. 1974a, *Ap. J.*, **187**, 231.
- _____. 1974b, *ibid.*, **192**, 29.
- _____. 1975, *ibid.*, **200**, 419.
- Rank, D. M., Townes, C. H., and Welch, W. J. 1971, *Science*, **174**, 1083.
- Solomon, P. 1973, *Physics Today*, **26**, 32.
- Solomon, P., and Klemperer, W. 1972, *Ap. J.*, **178**, 389.
- Spitzer, L., Drake, J. F., Jenkins, E. B., Morton, D. C., Rogerson, J. B., and York, D. G. 1973, *Ap. J. (Letters)*, **181**, L116.
- Spitzer, L., and Tomasko, M. G. 1968, *Ap. J.*, **152**, 971.
- Walmsley, C. M. 1973, *Astr. and Ap.*, **25**, 129.
- Watson, W. D. 1973, *Ap. J. (Letters)*, **183**, L17.
- _____. 1974a, *Ap. J.*, **188**, 35.
- _____. 1974b, *ibid.*, **189**, 221.
- Watson, W. D., and Salpeter, E. E. 1972, *Ap. J.*, **175**, 659.
- Werner, M. 1970, *Ap. Letters*, **6**, 81.
- Witt, A. N., and Lillie, C. F. 1973, *Astr. and Ap.*, **25**, 397.
- York, D. G., Drake, J. F., Jenkins, E. B., Morton, D. C., Rogerson, J. B., and Spitzer, L. 1973, *Ap. J. (Letters)*, **182**, L1.

WILLIAM LANGER: Institute for Space Studies, Goddard Space Flight Center, NASA, 2880 Broadway, New York, NY 10025